

DETECTION OF FLAWS IN CLOSE PROXIMITY USING CONVOLUTIONAL NEURAL NETWORKS

Arthur Chapon¹

École de Technologie Supérieure
Montréal, QC, Canada

Pierre Bélanger

École de Technologie Supérieure
Montréal, QC, Canada

ABSTRACT

The ability of an ultrasonic testing method to distinguish flaws in close proximity relative to the wavelength is limited by the theoretical resolution limit. Ultimately the reflections become superposed in the same wave packet. In many ultrasonic testing scenarios, the maximum useable frequency is limited by attenuation, and it may therefore become difficult to detect flaws in close proximity and impossible to increase the frequency. The purpose of this work is to use a convolutional neural network in order to separate and identify the time of arrival overlapping echoes. The machine learning algorithm was trained using finite element simulations and was then tested on experimental measurements. The convolutional neural network was able to distinguish shallow flat bottom hole in an aluminum block with a depth corresponding to only 0.5λ .

Keywords: Ultrasound, Resolution, Time-of-Flight, CNN, Imaging

1. INTRODUCTION

In ultrasonic non-destructive evaluation, a tradeoff must be made between the resolution and the propagation distance. Indeed, increasing the frequency increases the resolution but also the attenuation, and thus decreases the practical depth of the measurement. When the maximum useable frequency is low, overlapping echoes of defects and the backwall rapidly becomes a problem. Methods using deconvolution exist and have good results in simulation but are disappointing in practice [1].

The use of Convolutional Neural Network (CNN) in signal processing has thus far been studied mainly for classification purposes [2, 3]. Pre-processing methods such as the discrete wavelet transform or the 1-D LBD algorithm were implemented to help the machine-learning algorithms gain accuracy in the classification.

In this paper, a new method of Time-of-Flight (ToF) picking based on a CNN is proposed. The algorithm locates pattern

echoes from reflectors, even when the SNR is low or when the reflectors are in close proximity. The neural network is trained and validated with simulations generated with the GPU-accelerated finite elements code Pogo [4]. The CNN is then used to deconvolve experimental signals acquired on a block of aluminum with machined flat bottom holes.

2. MATERIALS AND METHODS

2.1 Simulations

In CNN, the larger the training and validation data sets are, the higher the accuracy of the neural network tends to be. Hence, provided that simulations are accurate, they are the most efficient solution to train a CNN. However, the difficulty is to ensure that the simulations and experiments are in excellent agreement.

Finite element (FE) simulations of the propagation of ultrasonic guided waves have been used successfully for a number of years. At 15 elements per wavelength, standard FE codes are typically too slow to be considered in the training of a CNN. However, simulation codes recently saw a rapid acceleration with the advent of graphics processing unit (GPU). GPU accelerated simulation codes enables the simulations of a large number of cases in a limited amount of time.

In this paper, the material was arbitrarily chosen as aluminum. However, the results presented in this paper could be easily transposed to other materials. The speed of sound of the experimental block was measured to ensure a perfect fit with the simulations. 2D simulations were considered due to their lower computational cost. 3D models offer a higher fidelity to experiments but are significantly more expensive in terms of computation time. Figure 1 presents a schematic of the parameterized finite element model.

¹ Contact author: arthur.chapon.1@ens.etsmtl.ca

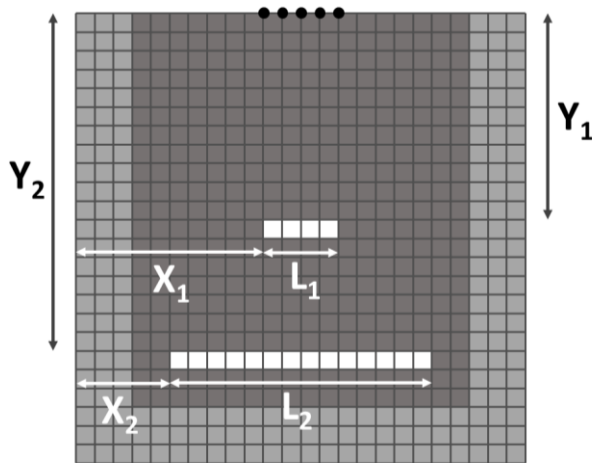


FIGURE 1: SCHEMATIC AND PARAMETRISATION OF THE FE MODEL USED FOR SIMULATIONS.

Absorbing boundaries were used to simulate an infinite block and therefore reduce the number of degrees of freedom of the model. In the model, the reflectors, in white, correspond to deleted elements. The black dots show the excited nodes. The positions (X_1 , X_2 , Y_1 and Y_2) and the dimensions (L_1 and L_2) of the two flaws were random. L_1 was also chosen to be always shorter than L_2 to avoid shadowing effect. The depth of the two flaws were stored in memory.

2.2. Convolutional Neural Network

Among the diversity of artificial neural networks the CNN caught attention because of its ability to take account the temporal organization of an A-scan.

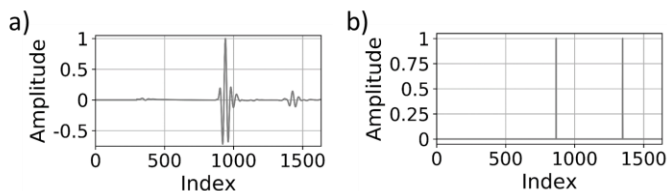


FIGURE 2: a) SIMULATED A-SCAN USED FOR TRAINING AND VALIDATION. b) TARGETED OUTPUT USED IN THE TRAINING OF THE CNN.

There are several advantages to CNN. Firstly, the algorithm can self-learn the statistical noise and the pattern of interest in the signal concurrently, without any operation of extraction. Secondly, the number of different self-learnt filters limits the impact of noise or the modifications of the echo patterns by scattering. Finally, CNN are able to learn pattern using time domain A-Scans.

The CNN used in this study only contains two 1D convolutional layers and can therefore be trained rapidly. A stochastic gradient descent is used to minimize mean squared error loss function. The learning rate was initially 0.05 and decrease logarithmically with the epochs. The learning stopped when 750 epochs were computed.

One thousand simulated A-scans were generated. The first 750 were the training set, the next 200 were used as the validation batch and the last 50 were used to evaluate the trained CNN. The evaluation of the trained CNN was only done in simulations at this stage and therefore didn't take into account the experimental effects.

2.3. Experiments

An aluminum block was used to verify the efficiency of deconvolution using a CNN trained with simulations. 26 flat bottom holes (FBH) were machined with decreasing depth. The CNN was then used to distinguish the reflection from the backwall and the FBH. The accuracy of the algorithm was evaluated by comparing the distance between the reflectors as evaluated by the CNN with the true distance. An Olympus probe V125 RM was used in pulse-echo with a centre frequency of 2.25 MHz. Signals were acquired with a Verasonics Vantage 64 LE data acquisition system with a sampling frequency of 25 MHz.

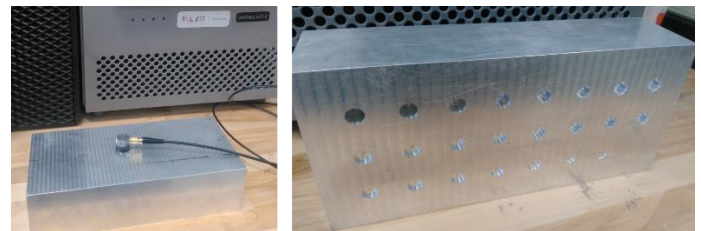


FIGURE 3: ALUMINUM BLOCK USED IN THE VALIDATION OF THE CNN.

Before the generation of training data, five A-scans were measured on the aluminum block so as to extract backwall echo patterns. The echoes were used to estimate the speed of sound in the aluminum block as well as the bandwidth of the transducer. Those parameters were then used in the simulations. For the validation of the CNN, 54 A-Scans or 2 for each FBH were then acquired.

3. RESULTS AND DISCUSSION

The CNN was applied on the experimental A-scans. Two examples of results are shown below in figures 4 and 5. In Fig. 4., the distance between the flat bottom hole and the backwall was 0.69 mm (or 0.25λ) therefore corresponding to a separation on the A-Scan of 0.5λ at 2.25 MHz. The wave packet in the A-Scan appears to contain only one reflector but the CNN was able to distinguish a pair of reflectors in close proximity. This case was the limit for which the CNN was still able to distinguish two reflectors and also corresponds to the theoretical resolution limit. Although the FBH was detected, its position in the deconvolved A-Scan was 1.27 mm instead of 0.69 mm.

Fig. 5. presents another example for which the distance between the reflectors was 2.06 mm or 0.74λ and corresponding to 1.48λ on the A-Scan at 2.25 MHz. In this case, the wave packet does appear to contain more than one reflector but the CNN is able to detect the position of the reflectors. In this case, the

deconvolved A-Scan shows a distance between the reflectors of 2.76 mm instead of 2.06 mm. A similar trend was seen on other measurements: as the FBH becomes deeper the error on the position decreases. This error is not related to the speed of sound in the material because the backwall also appears at the right position in the deconvolved A-Scans.

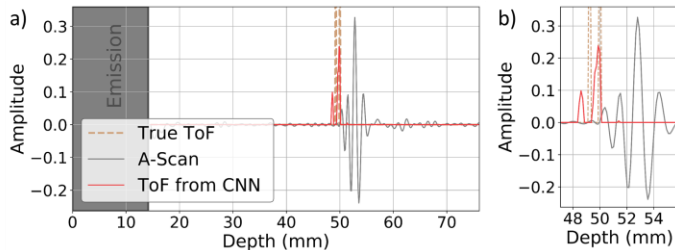


FIGURE 4: a) A-SCANS, EXPECTED TIME OF ARRIVAL AND OUTPUT OF THE CNN WHEN THE REFLECTORS ARE 0.69 MM APART (0.5λ AT 2.25 MHz). b) ZOOM ON THE REGION OF INTEREST.

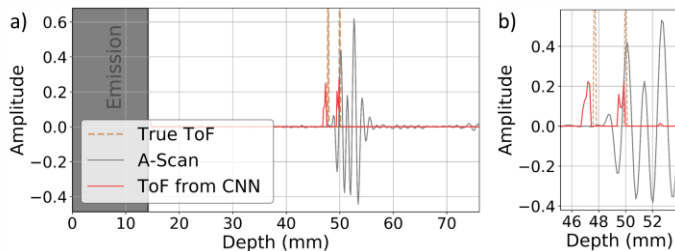


FIGURE 5: a) A-SCANS, EXPECTED TIME OF ARRIVAL AND OUTPUT OF THE CNN WHEN THE REFLECTORS ARE 2.06 MM APART (1.48λ AT 2.25 MHz). b) ZOOM ON THE REGION OF INTEREST

4. CONCLUSION

In this study, a CNN was used to deconvolve experimental A-Scans. The CNN was trained using only FE simulations. The trained CNN was then able to deconvolve reflectors separated by 0.5λ at 2.25 MHz therefore reaching the theoretical limit. With a reflector separation of 0.5λ , the A-Scan appears to contain only one reflector but the CNN is able to distinguish two reflectors. The estimation of the position of the reflectors is not quite accurate as it always overestimate the distance between the reflectors. The overestimation reduces when the distance between the reflectors increases.

ACKNOWLEDGEMENTS

We would like to thank Nvidia for providing us with a Nvidia Quadro P6000 graphics card for our GPU simulations. The authors would also like to thank the Natural Sciences and Engineering Research Council of Canada for funding this project by the oN DuTy! program.

REFERENCES

- [1] Ewen Carcreff, Sebastien Bourguignon1, Jérôme Idierl and Laurent Simo. “Resolution enhancement of ultrasonic signals by up-sampled sparse deconvolution”, 2013 IEEE International Conference on Acoustics, Speech and Signal Processing, Vancouver, BC, Canada, May, 26-31, 2013. DOI: 10.1109/ICASSP.2013.6638920
- [2] Virupakshappa, Kushal, Marino, Michael and Oruklu Erdal. “A Multi-Resolution Convolutional Neural Network Architecture for Ultrasonic Flaw Detection”, 2018 IEEE International Ultrasonics Symposium, Kobe, Japan, October 22-25, 2018. DOI: 10.1109/ULTSYM.2018.8579888
- [3] Hu, Hongwei, Peng, Gang, Wang, Xianghong and Zhou, Zhenhua. “Weld defect classification using 1-D LBP feature extraction of ultrasonic signals”, *Nondestructive Testing and Evaluation* Vol. 33 No. 1 (2018): pp. 92-108. DOI: 10.1080/10589759.2017.1299732.
- [4] Huthwaite, Peter “Accelerated finite element elastodynamic simulations using the GPU.” *Journal of Computational Physics*, Vol 257, (2014): pp. 687–707. DOI: 10.1016/j.jcp.2013.10.017.